Pre-Series Sensor Qualification for the Inner Tracker of LHCb

G. Baumann[1], D. Boeni[1], L. Buchmann[1], A. Büchler[1], N. Chiapolini[1], E. Eisenring[1], A. Landwehr[1], F. Lehner[1], C. Lois[1,2], T. Mattle[1], T. Müller[1], S. Nüesch[1]

[1] *Physik-Institut der Universität Zürich, Switzerland*

[2] *Universidade de Santiago de Compostela, Spain*

Abstract

This note gives a description of the sensors that will be employed in the Inner Tracker of LHCb, and presents the results on sensor qualification for the pre-series production, manufactured by Hamamatsu Photonics.

1 Introduction

The "Inner Tracker" (IT) [1] is part of the tracking system of the LHCb experiment [2]. It consists of three tracking stations downstream of the spectrometer magnet of the experiment and covers a cross-shaped area around the beam pipe. Each station consists of four independent detector boxes, above, below and to both sides of the beam pipe, each with four planar detection layers that will be covered by silicon micro-strip detectors. One-sensor modules built using 320 μm thick silicon micro-strip detectors are used in the top/bottom boxes, and two-sensor modules built using 410 μm thick silicon micro-strip detectors will be used in the left/right boxes.

A total of 504 sensors will be employed in the IT stations. They have to be tested to ensure their functionality and check whether they pass the specified acceptance criteria.

The two types of IT sensors are identical apart from their different thicknesses. The detectors are single-sided p-on-n type, AC coupled sensors, produced from 6" wafers. The physical dimensions of the sensors are 78 mm $\times$ 110 mm. The p^+ strip pitch is 198 μm and the implant width is 50 μm, which

Table 1: Geometry parameters and characteristics of the sensors.

Wafer size	6”
Overall width	(78 ± 0.005) mm
Nominal thickness HPK-320	(320 ± 10) μm
Nominal thickness HPK-410	(410 ± 10) μm
Wafer flatness	± 25 μm
Cutting line parallelity	± 5 μm
Overall length	(110 ± 0.005) mm
Minimum active strip length	108 mm
Bulk material	n type
Implant	p^+ type
Crystal orientation	$\langle 100 \rangle$
Pitch	(198 ± 1) μm
Implant width	(50 ± 1) μm
# of strips	384
Biasing	polysilicon
Read-out coupling	AC

results in a w/p ratio of 0.25. The width of the metal strips is 58 μm (8 μm wider than the implant strips), which gives rise to a more stable operation with respect to high bias voltages. The nominal thickness of the n-type substrate is 320 μm for the from now on called HPK-320 sensors, and 410 μm for the so-called HPK-410 sensors. Further details can be found in [3, 4].

The sensors are manufactured by Hamamatsu Photonics (HPK). The total production will comprise 580 sensors: 194 HPK-320 sensors and 386 HPK-410 sensors. A pre-series production of 60 sensors was ordered, out of which 49 sensors were delivered: 14 HPK-320 and 35 HPK-410 sensors. According to the company, they underestimated the production yield and were not able to send the remaining sensors on time, shifting the missing sensors from the pre-series production to main production. As a compensation, 12 mechanical pieces (without implants) and 3 lower-grade sensors (visually bad) were sent to us for free. The sensors were received at CERN and then shipped to Zürich for testing.

The outline of this note is the following. In Section 2, a brief summary of the tests performed by the vendor is presented. In Section 3, results from the visual inspection and metrology tests, as well as measurements of leakage current, depletion voltage and coupling capacitance are described. In Section 4, the conclusions of our measurements are presented.

Table 2: Specifications and acceptance criteria of the sensors.

Total leakage current	< 1 μA at V_{depl}+100 V
Individual strip current	< 10 nA at V_{depl}+100 V
Breakdown voltage	> 500 V
Full depletion voltage	50-140 V
Coupling capacitance	> 60 pF/cm
Total strip capacitance	< 1.6 pF/cm
Bias resistors	(1.5 ± 0.5) MΩ
Bad strips per sensor	< 4

2 Vendor results: HPK tests

HPK tests the sensors prior to shipment in order to verify that they pass the acceptance criteria. HPK provides us with the results of these tests, which include leakage currents up to 500 V, full-depletion voltages, strip currents, and sensor thickness on every sensor. For a random sample per wafer lot we receive information on polysilicon resistors, coupling capacitances, breakdown voltage of capacitors, and implant resistances. In addition, HPK provides a list of bad strips. According to their results, all sensors have leakage currents below 1 μA at 500 V and the remaining electrical parameters are within specification as well. Out of the 49 delivered sensor, there are only two sensors with one bad strip each (one leaky strip and one strip with a pinhole in the coupling capacitor).

As an example[1], the strip currents at 250 V for two sensors with typical profiles are shown in Figure 1. The strip currents are very small for all sensors and out of the 49 sensors only one strip was leaky drawing ~ 230 nA at 250 V. The strip currents for all pre-production sensors can be found at [5].

3 Sensor quality control and results from the pre-production testing

The first 49 IT pre-production sensors were received and tested in Zürich in January 2005. In this section, we describe the quality assurance tests that were performed on the sensors, together with the results of our measurements.

[1]Strip currents are selected as example since we did not measure them.

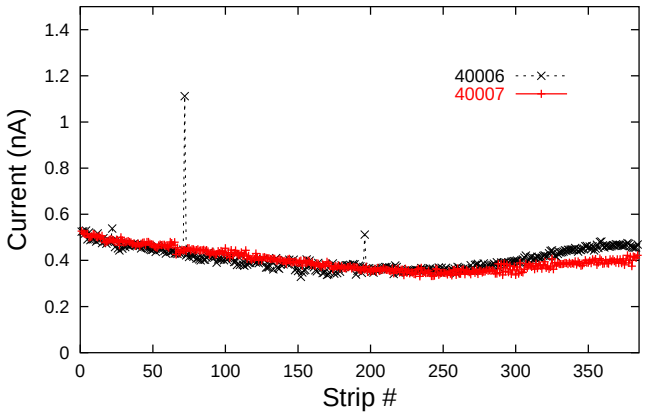

Figure 1: Strip currents measured at 250 V by HPK for two HPK-410 sensors.

3.1 Visual Inspection

A visual inspection was performed on all sensors in order to search for macroscopic defects. This is an important test, since large defects are easily detected and can give rise to instabilities in the electrical behaviour of the sensors or an increase of the leakage currents. First, an overall inspection of the strip side and the backplane was performed by eye and using a magnifying glass. Then, the strip side full surface was inspected under a microscope, taking note of scratches and defects, looking for chipped edges, pad bondability or contamination, as well as checking for the overall cleanliness of the sensors. In addition, the serial number on the scratch-pad was checked to be the same as that marked on the envelope.

According to the observed defects, a grading procedure was developed:

- Sensors without deep scratches or chips, and without pad contamination, were classified as A grade.
- Sensors with some superficial scratches (not deep enough to break strips), or slightly chipped edges, or acid damage in less than four strips, or a combination of these, were classified as B grade.
- Sensors with chipped edges, or deep scratches, or acid damage in more than four strips, or damaged pads, were classified as C grade.
- Sensors with long and deep scratches or chips, or extremely dirty, were classified as D grade.

Table 3: Number of sensors according to the visual inspection grade.

Visual Grade	Number of sensors	
	HPK-320	HPK-410
A	12	24
B	2	11
C	-	-
D	-	-

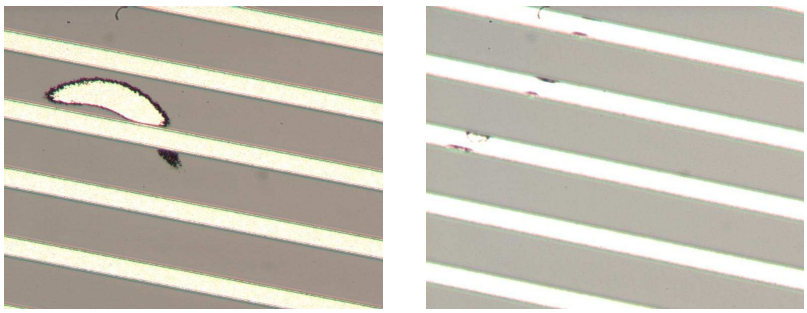

Figure 2: Examples of the defects found on sensors that were classified as B grade in the visual inspection. On the left, excess of aluminium between two strips. On the right, chipped strips.

In Table 3, the number of sensors according to the visual grading is shown. No deep scratches or big defects were found. About 65% of the sensors were free of defects and classified as A grade sensors. All remaining sensors were classified as B grade. A and B grade sensors can both be used to build silicon modules for use in the experiment.

Some examples of the observed defects, like an excess of aluminium between two strips, or a few slightly chipped strips are shown in Figure 2.

3.2 Leakage currents

The leakage current is the reverse current of the *pn*-junctions. It gives rise to a background noise and is caused by thermally excited minority carriers that are generated in the depleted region and, due to the electric field, drift to the electrodes. For a given bias voltage, the size of the leakage current depends to a certain extent on environmental factors, like temperature, humidity and time of operation of the sensor, but its variation will in general be small (of

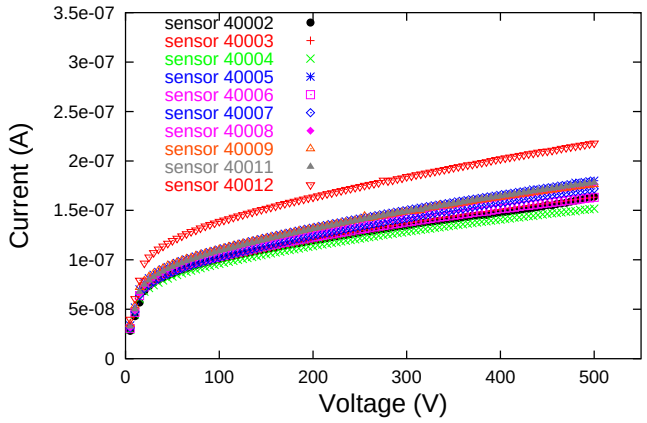

Figure 3: Typical IV curves measured on the HPK-410 sensors. No breakdown is observed below 500 V.

the order of a few 100 nA at the full depletion voltage for a good sensor).

In this section, results on leakage currents for the 49 IT pre-series sensors are presented, and typical IV curves are shown. The leakage current dependence on the application of vacuum to the chuck of the probe station is investigated, and the stability and repeatability of the currents are studied.

The current between the backplane and the bias ring was measured for all sensors as a function of the reverse bias voltage, using a Keithley 487 unit (picoamperemeter + voltage source). The bias voltage was increased in steps of 5 V up to 500 V, over a period of 5 minutes. The measurements were performed at room temperature, typically about 20℃, and at a relative humidity below 30%.

A great uniformity of the currents from sensor to sensor was found. As an example, typical IV curves are shown in Figure 3 for ten HPK-410 sensors. The currents were found to be very low, typically below 300 nA at 500 V. Only one of the sensors had higher leakage current, about 900 nA at 500 V, due to the presence of one leaky strip. None of the sensors evidenced breakdown below 500 V [2].

It had been observed [6] that the leakage currents for sensors produced by other companies depended critically on the application of vacuum to hold the sensors to the chuck of the probe station. To check for a possible effect on the HPK sensors, the leakage currents of 15 sensors were re-measured

[2]Two of the lower-grade sensors supplied as free samples were tested up to higher voltages, and they evidenced breakdown at about 800 V.

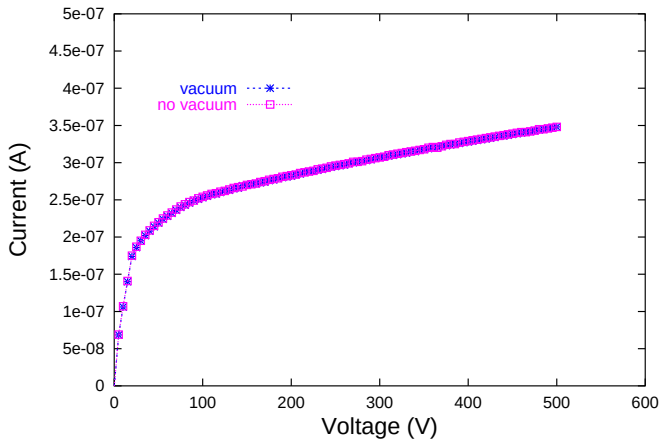

Figure 4: Leakage currents measured with and without chuck vacuum for sensor HPK-410 40027. The currents do not depend on the application of vacuum to the chuck.

without chuck vacuum. No difference between the currents obtained with and without chuck vacuum was observed for any of the sensors. As an example the measured curves for one of the tested sensors are shown in Figure 4.

The repeatability of the IV curves under stable conditions (same strain, temperature and relative humidity) was checked for $\sim$ 10% of the sensors. About 30 IV curves on each sensor were taken, waiting for 35 min between two consecutive measurements. Figure 5 shows as an example the 30 IV curves obtained for one HPK-410 sensor. The IV curves were found to be highly reproducible.

Moreover, the current stability of 10% of the sensors was investigated in a $\sim$ 30 h long biasing test, while temperature and relative humidity were monitored. The leakage currents were stable and reproducible against long term drifts. Only small drifts in current were observed and these were correlated to temperature, as shown in Figure 6.

A comparison was made between the currents that we measured and the data provided by HPK. We found currents slightly lower than the values quoted by HPK. Typically, we measured leakage currents of about 150-300 nA at 500 V, whilst HPK measured leakage currents of 250-450 nA at the same voltage. We assume that this difference is due to differences in the setup or ambient conditions.

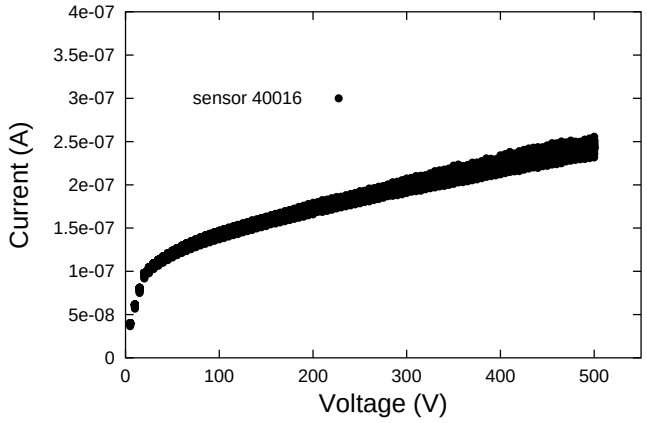

Figure 5: Leakage currents taken for sensor HPK-410 40016 as a test of repeatability. The 30 IV curves shown in the plot were taken during night, waiting 35 minutes between them.

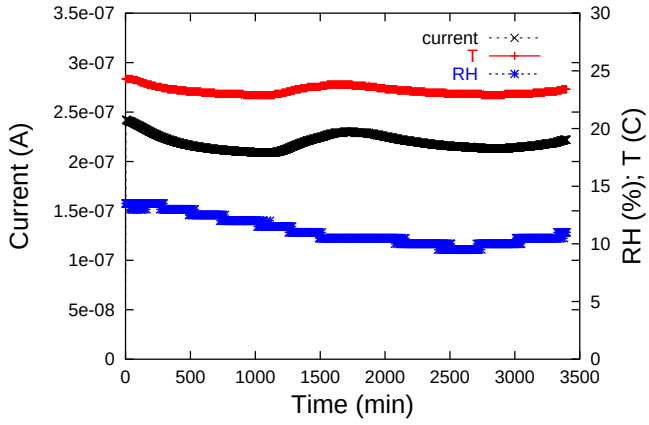

Figure 6: Current stability test for sensor HPK-320 30004. The sensor was biased at 450 V during 58 hours. The relative humidity (RH, lower curve) and temperature (T, upper curve) are plotted to show the evolution of the ambient conditions.

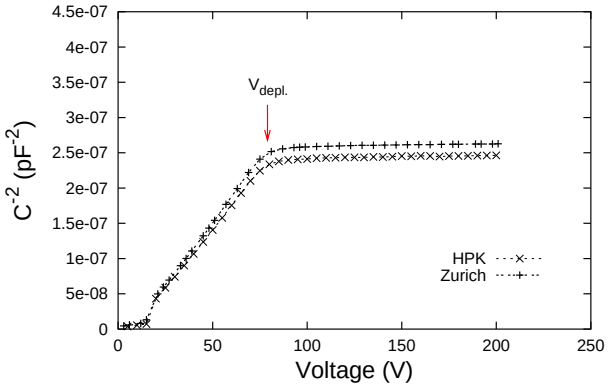

Figure 7: Determination of the full depletion voltage from the measurement of $1/C^2$ as a function of the bias voltage. The depletion voltage is determined as the intersection of two straight lines and is indicated by the arrow. Shown is a typical curve, corresponding to sensor HPK-410 40005. The curve measured by the vendor was added to show the reproducibility of the data.

3.3 Depletion Voltage

The full depletion voltage determines the operation voltage of the sensors. Therefore, it is a very important information for module assembly, since sensors should be matched in depletion voltage when they are mounted on the same module. We estimated the full depletion voltage from the measurement of the bulk capacitance as a function of the applied bias voltage. The bulk capacitance of the sensor is the capacitance of all readout strips to the backplane. It is proportional to the inverse of the square root of the bias voltage applied to the sensor until full depletion is reached, and then assumes a constant value. We plot $1/C^2$ as a function of the bias voltage and estimate the depletion voltage as the intersection of two straight lines fitted to the rising part and the flat part of the curve, respectively.

The capacitance measurements were performed on all sensors, using a Keithley 487 unit as a voltage source and an HP 4192 LCR meter to measure the capacitance between the bias line and the backplane. The CV curves were measured using a signal frequency of 1 kHz and a signal amplitude of 1 V. Figure 7 shows a typical curve of $1/C^2$ as a function of the bias voltage. The measurements performed by HPK are included to demonstrate the reproducibility of the data.

Figure 8 shows the distribution of the full depletion voltages for all sensors. All of them are between 70 and 140 V, fulfilling our specifications.

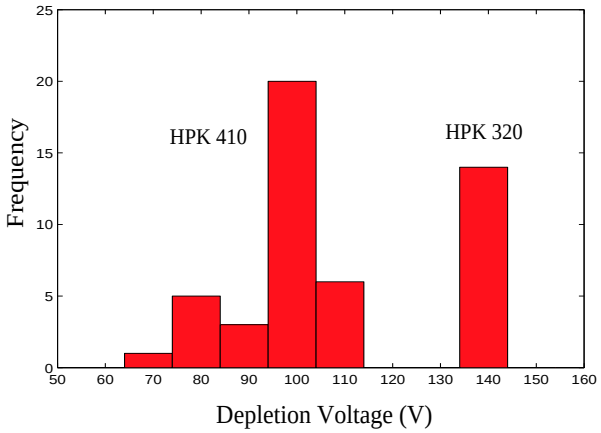

Figure 8: Distribution of the measured full depletion voltages. All the sensors deplete between 70 and 140 V, fulfilling the specifications.

In addition, we estimated the full depletion voltages using the method followed by HPK. In this method, the full depletion voltage is considered to be the voltage at which $1/C^2$ decreases by 4% with respect to its value in the *plateau*. In Figure 9, the results obtained using this method (method 2) are compared to those obtained from the intersection of two straight lines (method 1). The results using the two methods are in excellent agreement. A comparison between the full depletion voltages that we determined using method 2 and the data provided by HPK is shown in Figure 10. Very good agreement between both data sets can be observed.

3.4 Tests with automatic probe station

The coupling capacitance is the capacitance between the strip implant and the read-out aluminium line. Its measurement allows to detect certain classes of bad strips, which are characterized by a metal open, a metal short or a pinhole in the dielectric substrate of the coupling capacitor.

Coupling capacitance measurements were performed using an Electroglas 1034XA6 automatic probe station equipped with a probe card to simultaneously contact AC- and DC- pads on a given strip, and an HP 4192A LCR meter. The probe station and the LCR meter were controlled via GPIB bus by Labview programs running on a PC. The measurements were taken at a signal frequency of 1 kHz and a signal amplitude of 1 V [7].

The measurements were carried out on about 20% of the pre-production sensors and on the three lower-grade sensors provided by HPK. An example

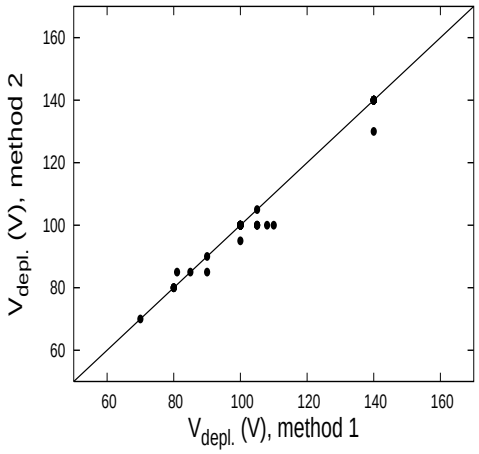

Figure 9: Comparison between the full depletion voltages estimated as the intersection of two straight lines (method 1) and as the voltage at which $1/C^2$ decreases by 4% with respect to its value in the *plateau* (method 2).

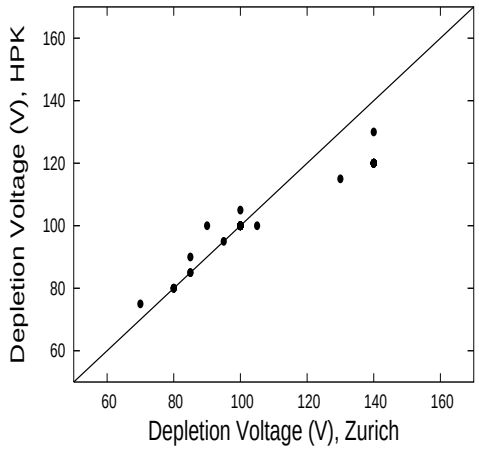

Figure 10: Comparison between the full depletion voltages measured by HPK and our measurements (using method 2). Excellent agreement between both data sets is observed.

Table 4: List of strips flagged as containing pinholes or capacitor values out of specification by HPK, and strips flagged as bad in our set up.

Sensor ID	Bad strips (Zürich)	Bad strips (HPK)	
		Pinholes	Bad Capacitor
30002	196	196	-
40027	-	269	-
40037 (low-grade)	321, 320	-	321, 320

of the obtained coupling capacitance profile is shown in Figure 11. One of the strips has coupling capacitors out of specification due to pinholes in the oxide. The bad channels observed in our coupling capacitor scans are listed in Table 4 together with the list of bad strips provided by HPK. Out of the total of 5376 inspected strips, four strips were flagged as bad by HPK as containing pinholes or having capacitance values out of specification. Out of these, we could detect three. We could not verify one strip flagged as pinhole. We did not find any bad strip in addition to those flagged as bad by HPK.

The number of defective strips is specified to be less than four per sensor. All inspected sensors were below this number.

3.5 Total strip capacitance

The total strip capacitance is here defined as the sum of the capacitance to the backplane and the capacitance to adjacent strips, measured at a signal frequency of 1 MHz [8]. The effect of the remaining strips was neglected in view of the large pitch of the sensors. The two closest neighbours were AC coupled to the backplane. A sketch of the measurement setup can be seen in Figure 12.

The interest in these measurements lays in the fact that the total strip capacitance limits the achievable signal-to-noise ratio of a sensor connected to fast read-out electronics, since the Johnson noise from the load capacitance at the input of the pre-amplifier is the main contribution to the noise of the front-end amplifier.

Measurements of the total strip capacitance as a function of the bias voltage were carried out for six strips of two lower-grade HPK-410 sensors, and for two strips of the baby-detectors contained in two HPK-320 test-structures. Figure 13 shows an example of this dependance for one strip of sensor HPK-410 40001. The obtained capacitance values, at bias voltages above the full depletion voltage, are summarized in Table 5. The mean value

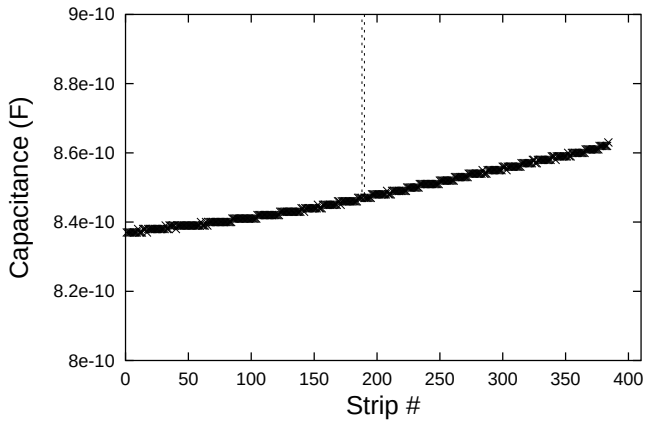

Figure 11: Coupling capacitance as a function of the strip number for sensor HPK-320 30002. Strip 196 has a coupling capacitance of 2 mF, which is out of specifications and lays out of the scale of this plot. This is a typical profile of the coupling capacitors across the sensor, which is likely to be related to process inhomogeneities.

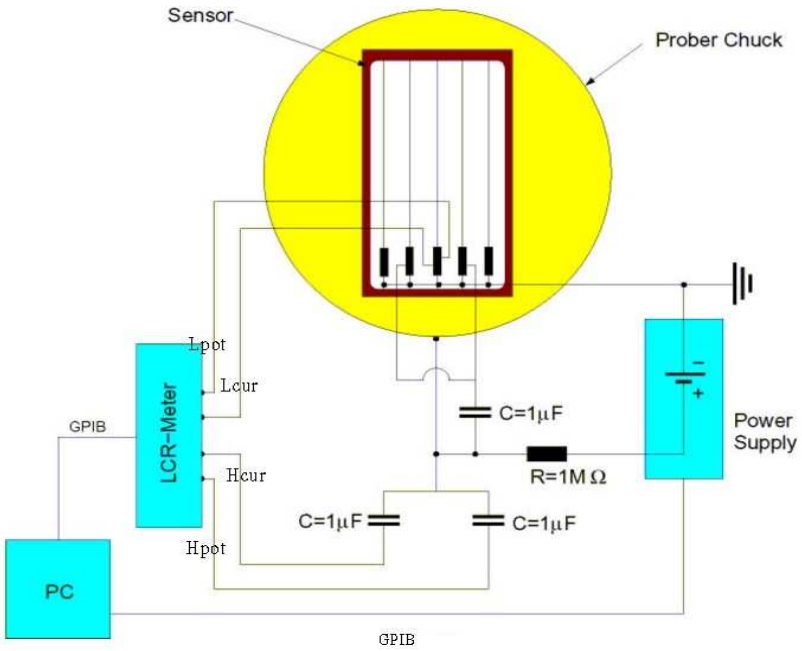

Figure 12: Setup for the total strip capacitance measurements.

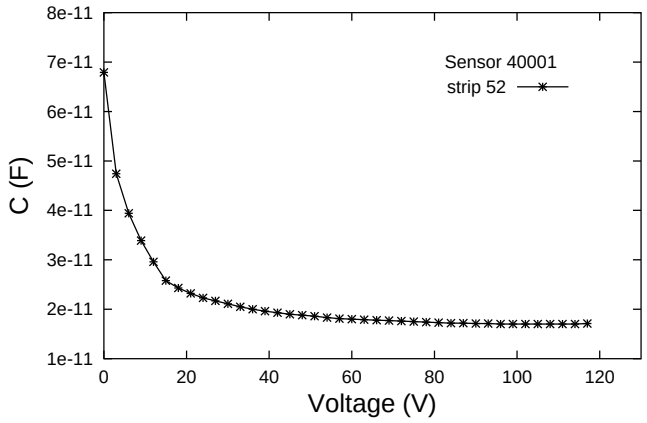

Figure 13: Total strip capacitance as a function of the bias voltage for one strip of sensor HPK-410 40001.

was calculated for each sensor and the error assigned to it corresponds to the RMS of the individual measurements for this sensor.

3.6 Metrology

Metrological measurements were performed on all sensors in order to determine the warp of the sensors and to verify the cutting line precision and parallelity, as well as other geometrical features on the sensors. We measured the diameter of the alignment marks on the sensors, the distance between them, the parallelity between edges, the width of the guard ring, bias ring and selected strips, the distance between the edges and the guard ring, bias ring and selected strips, the overall length and width of the sensor, the distance between consecutive strips, the parallelity between edges and strips, and flatness. The metrology grading procedure was based only on some of them: flatness, overall length and width of the sensor, distance between the edge and the strips, and parallelity between the edges and the strips. All sensors were mechanically classified as A grade. The parallelity and precision of the cut edges are important due to the proposed module assembly procedure [9], which exploits the accuracy of the dicing edge of the sensors for alignment purposes. In an assembly template, the sensors are pushed with their cut edges against positioning pins in order to align them with respect to each other and with respect to alignment pins in the module support. According to the specifications, the sensor warp should be less than 50 μm, and the cutting line parallelity should be better than 10 μm.

Table 5: Total strip capacitance for two lower-grade HPK-410 sensors and for two baby-detectors contained in HPK-320 test-structures. The mean value of the capacitance on each sensor and the mean capacitance normalized by the strip length are included. The errors correspond to the RMS of the data.

Sensor ID	Strip	C (pF)	$\overline{C}$ (pF)	$\overline{C}$/L (pF/cm)
40001	# 1	16.6	16.8 ± 0.7	1.56 ± 0.06
	# 2	17.6		
	# 3	15.6		
	# 4	16.7		
	# 5	17.3		
	# 6	17.1		
40010	# 1	16.3	17.2 ± 0.9	1.59 ± 0.08
	# 2	17.2		
	# 3	17.3		
	# 4	17.2		
	# 5	16.4		
	# 6	18.8		
Test-structure 30012	# 1	15.4	15.3 ± 0.2	1.42 ± 0.02
	# 2	15.1		
Test-structure 30013	# 1	16.1	15.6 ± 0.5	1.44 ± 0.05
	# 2	15.1		

Figure 14 shows the distribution of the measured overall width and length for the sensors. On average, the sensors are 9 μm longer and 6 μm wider than the nominal dimensions, which is actually outside the given tolerances. The sensor-to-sensor variation in width is however small, with a RMS of 1 μm and a full range of less than 5 μm. Variations in length are slightly larger but since this dimension is not critical for the construction of the detectors, one can argue that the specifications were unnecessarily tight and all sensors were accepted.

Figure 15 shows the distribution of the measured parallelities between the sensor symmetry axis and a selected strip. For each sensor, the coordinates of ten points along each edge were measured. By fitting them to straight lines, the edges were reconstructed, and from these the symmetry axis was determined. The same procedure was repeated for the selected strip. The assigned parallelity is $L \tan\theta$, L being length of the sensor edge and θ the angle between the reconstructed lines. The mean parallelity accuracy was determined to be ~ 1 μm.

The flatness of the sensors was determined by measuring a profile of the surface height of the sensor laying freely on a flat surface, with the strip side facing upwards. On each sensor, z-coordinates have been recorded on an equidistant grid of 6×6 points covering the full surface of the sensor. Typical examples of the obtained profiles for each type of sensors are shown in Figure 16. It shows a characteristic sensor deflection of 75 μm for the HPK-320 sensors and of 55 μm for the HPK-410 sensors over the full surface. The distribution of the measured warp for all inspected sensors is shown in Figure 17. The mean warp was determined to be ~ 85 μm for the HPK-320 sensors and ~ 40 μm for the HPK-410 sensors. The maximum measured warp was ~ 95 μm for the HPK-320 sensors and ~ 60 μm for the HPK-410 sensors. These values are outside the specifications, but this seems to be not a problem. Although more mechanical strain is induced on the sensors when the modules are built, it was demonstrated that this had no effect on the leakage currents.

3.7 Overall sensor grading

Depending on the results of the tests described above, an overall grading was assigned to each sensor. The sensors are classified according to the following criteria:

- Grade-A: good sensors, graded as A or B in the visual inspection, and leakage currents $I < 1$ μA at $V_{depl} + 100$ V, and less than two bad strips per sensor, and graded as A in the metrology tests.

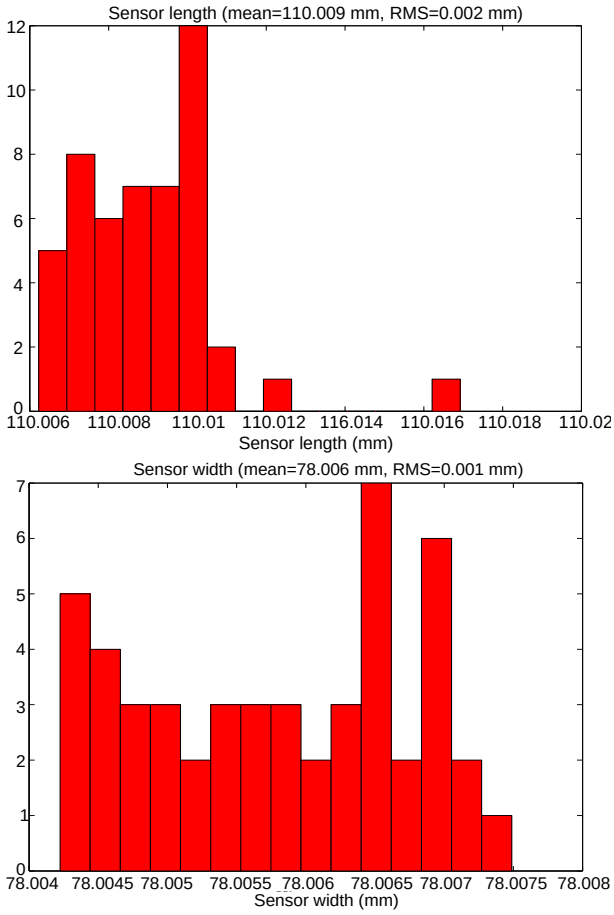

Figure 14: Distribution of the measured overall length (top) and width (bottom) for the 49 sensors. The mean length is 110.009 mm, and the mean width is 78.006 mm. The standard deviation from sensor to sensor is better than 2 μm.

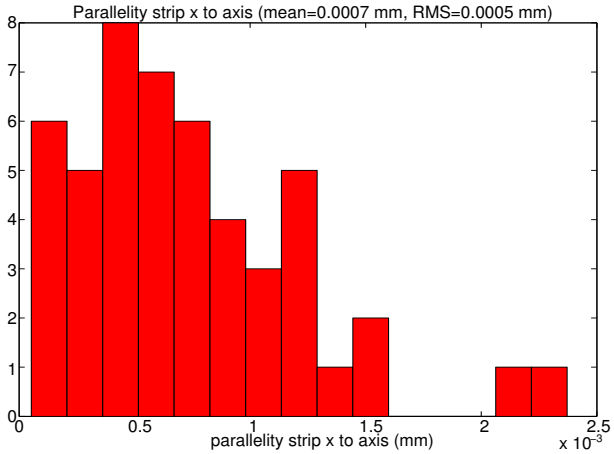

Figure 15: Distribution of the measured parallelities between the sensor axis and a selected strip.

- Grade-B: medium sensors, graded as B or C in the visual inspection, and leakage currents $I < 1$ μA at $V_{depl} + 100$ V, or between 2 and 3 bad strips per sensor, and graded as A in the metrology tests.
- Grade-C: poor sensors, graded as C or D in the visual inspection, or leakage currents $I \geq 1$ μA at $V_{depl} + 100$ V, or more than 3 bad strips per sensor, or graded as B in the metrology tests.
- Grade-X: destroyed.

Grade-A sensors should be used in the inner parts of the detector where particle densities are highest, whilst grade-B sensors could be used for the outer parts of the detector or as spares. Grade-C sensors should not be used, neither for the detector nor as spare. Concerning metrology measurements, leakage currents and number of bad strips, all tested sensors fulfill the requirements of grade A. After a re-evaluation of the visual grading, two out of the 49 tested sensors were given an overall grade B, whereas all other sensors were classified as grade A. No sensor was classified as grade C and no sensor was destroyed.

4 Conclusions

We have presented the results of sensor qualification for the pre-series production for the IT, produced by HPK. Our main results are the following:

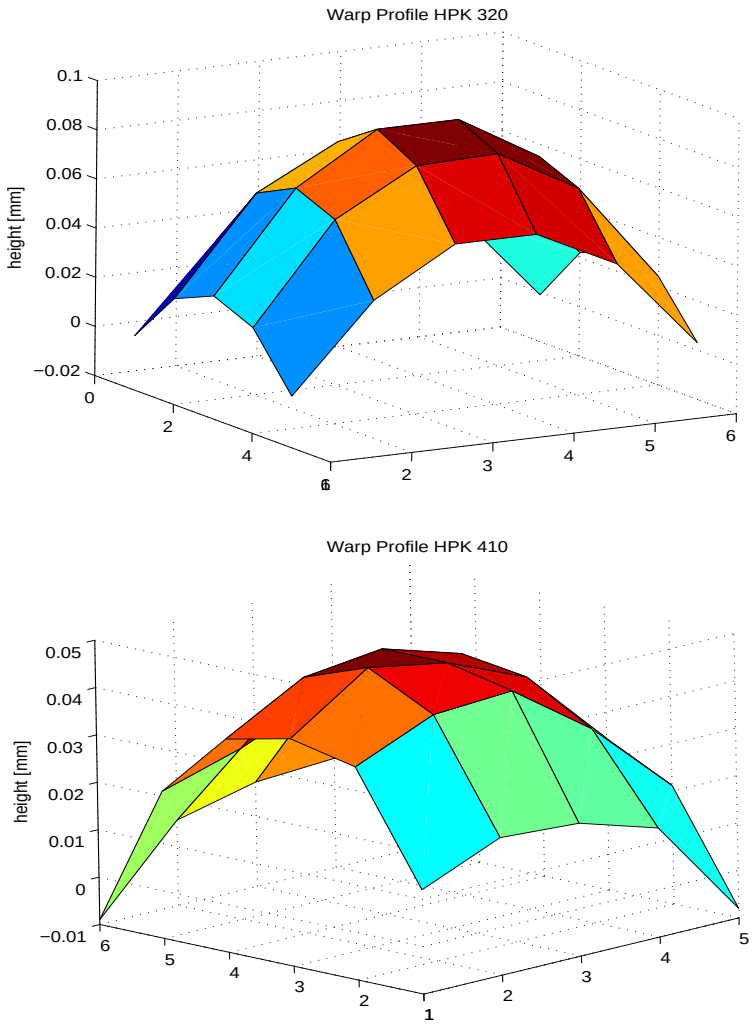

Figure 16: The z-profile of a sensor of each type is shown. The measured points are connected by surface grid lines. The z-coordinates were recorded on an equidistant grid of 6×6 points covering the full surface of the sensor.

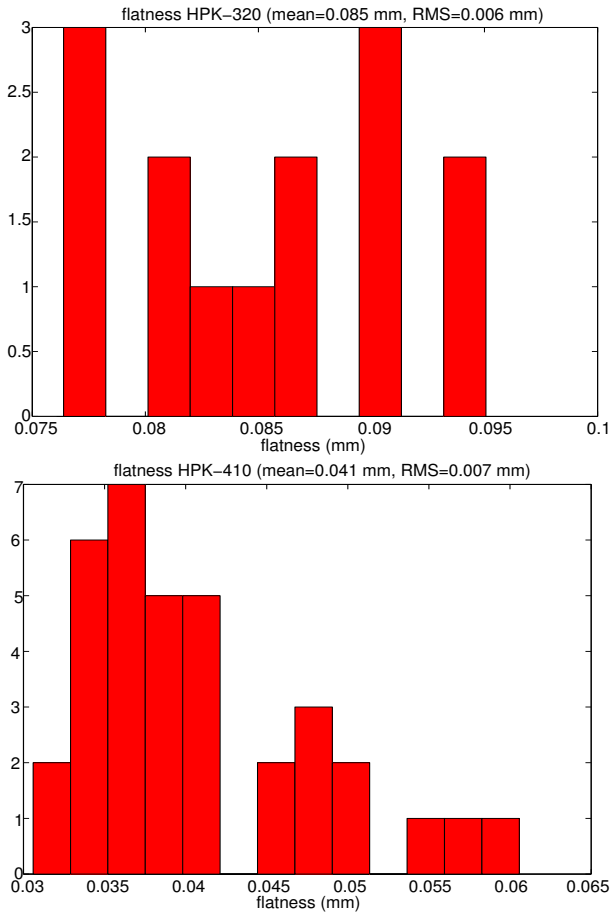

Figure 17: Distribution of the measured flatness on the HPK-320 sensors (top) and on the HPK-410 sensors (bottom).

- Visual inspection over all sensors was performed in order to detect macroscopic defects like scratches, chipped edges, pad contamination, as well as to check the cleanliness of the sensor. About 65% of the sensors were found to be free of defects, and all sensors were judged to be usable for detector production.

- Leakage current measurements were performed on all sensors. Currents were found to be very small, typically 300 nA at 500 V, and very similar from sensor to sensor. All sensors fulfill the leakage current specifications. None of the sensors evidenced breakdown below 500 V. Furthermore, the currents were found not to depend on the application of vacuum to the chuck of the probe station and were repeatable and stable over time of operation, as was verified on a sample of 15% of the sensor that were chosen randomly.

- Depletion voltages were measured for all sensors. All sensors fulfill the specifications, showing full depletion voltages in the range of 70-140 V.

- Coupling capacitance measurements were performed on 20% of the sensors using an automatic probe station. Out of the total of 5376 inspected strips, four strips were flagged as bad by HPK as containing pinholes or having capacitance values out of specification. Out of these, we could detect three. We could not verify one strip flagged as pinhole. We did not find any additional bad strip.

- Metrological measurements were performed on all sensors in order to determine the cutting line precision and parallelity, and the warp of the sensors, as well as other geometrical features. The mean warp was determined to be ~ 40 μm for the HPK-410 sensors and ~ 85 μm for the HPK-320 sensors, and the mean parallelity ~ 1 μm. The mean values of the sensor outer dimensions are within 9 μm of the nominal values. The standard deviation from sensor to sensor is better than 2 μm.

- According to the overall grading, two out of the 49 tested sensors were classified an grade B, whereas all other sensors were classified as grade A. No sensor was classified as grade C and no sensor was destroyed.

All sensors have been shipped to CERN, where the IT module production will take place.

References

[1] LHCb collaboration. *LHCb Inner Tracker Technical Design Report*. CERN/LHCC 2002-029.

[2] S. Amato et al. *LHCb Technical Proposal*. CERN-LHCC-98-4 (1998).

[3] F. Lehner and O. Steinkamp. *Specifications for the Inner Tracker Silicon Sensors* 320 μm *thick*. `http://ckm.physik.unizh.ch/tt/sensorprob/`.

[4] F. Lehner and O. Steinkamp. *Specifications for the Inner Tracker Silicon Sensors* 410 μm *thick*. `http://ckm.physik.unizh.ch/tt/sensorprob/`.

[5] `http://ckm.physik.unizh.ch/tt/sensorprob/`.

[6] G. Baumann *et al. Quality assurance of 100 CMS-OB2 sensors*. LHCb note 2004-105.

[7] F. Lehner, P. Sievers, O. Steinkamp, U. Straumann, A. Vollhardt, and M. Ziegler. *Description and Evaluation of Multi-Geometry Silicon Prototype Sensors for the LHCb Inner Tracker*. LHCb note 2002-038.

[8] F. Lehner, P. Sievers, O. Steinkamp, U. Straumann, and M. Ziegler. *Description and Characterization of Inner Tracker Silicon Prototype Sensors*. LHCb note 2001-036.

[9] J. Gassner, F. Lehner, and S. Steiner. *The Production, Testing and Assembly of the LHCb Silicon Trigger Tracker*. LHCb note 2004-109.